

Measurement of Beam Loading Effects in the High Pressure RF Cavity for Ionization Cooling

Moses Chung, Alvin Tollestrup, Andreas Jansson, and Katsuya Yonehara
Accelerator Physics Center, Fermi National Accelerator Laboratory, Batavia, IL 60510

(Dated: May 6, 2010)

The most serious problem expected in the beam test of the High Pressure RF (HPRF) cavity is the absorption of RF power by beam-induced electrons. In this note, we describe a simplified model for the beam loading effect that could be useful for experimental measurement.

I. INTRODUCTION

High Pressure RF (HPRF) cavity can be a very effective solution for the development of a compact muon ionization cooling system, such as Helical Cooling Channel (HCC). Initial experiments of HPRF cavity in the absence of the beam have demonstrated that higher field gradients are possible compared with the case of the conventional evacuated cavities. Figure 1 illustrates the typical breakdown limits observed in the experiments together with the proposed operation condition for HCC.

When beam is propagating through the HPRF cavity, however, there is some concern in relation with beam-induced electrons. If the beam-induced electrons are not removed properly, theory expects that significant amount RF power is dissipated by Ohmic heating and the cavity is heavily loaded. Detailed understanding and measurement of such beam loading effects are critical to evaluate the feasibility of HPRF cavity concept.

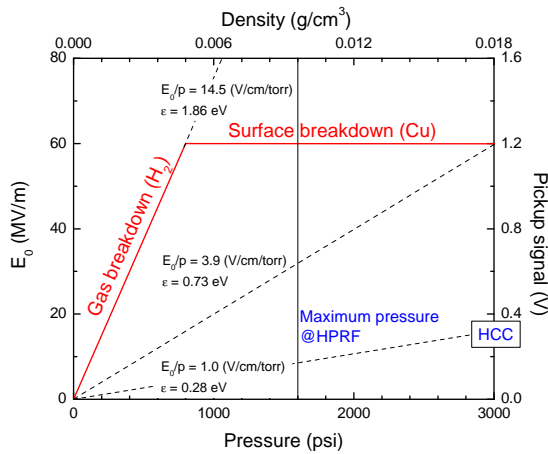


FIG. 1: Typical breakdown limits observed in the experiments without beam. The equilibrium energy ($\bar{\epsilon}$) of electrons in the hydrogen gas is determined by a single parameter E_0/p .

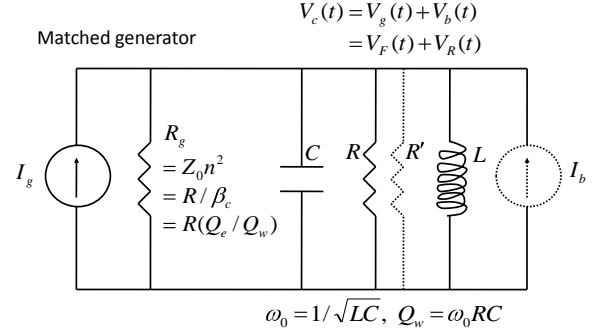


FIG. 2: Equivalent circuit for the beam-loaded cavity transformed into the resonator circuit. The quantity $R_g = R/\beta_c$ is the load impedance seen looking back toward the generator from the cavity. Here, $\beta_c = R/n^2 Z_0$ is the coupling coefficient, n is the turns ratio of the coupling, and Z_0 is the characteristic impedance of the waveguide. The RF power transfer from the generator becomes a maximum if the current flowing through the matched load impedance is $I_g/2$. For actual HPRF configuration, unfortunately, we don't have a matched load and a circulator that dissipate all backward waves.

II. EQUIVALENT CIRCUIT MODEL

The sources of the loading effects in the HPRF cavity can be divided into two; beam-induced image charges in the cavity surface and beam-induced electrons generated inside the cavity. Representing the effect of image charges by a current generator and the effect of electrons by an additional shut resistance (R'), we obtain the following approximate equivalent circuit equation (See Fig. 2):

$$\left\{ \frac{d^2}{dt^2} + \omega_0 \left(\frac{1}{Q_L} + \Delta \left[\frac{1}{Q} \right] \right) \frac{d}{dt} + \omega_0^2 \right\} V_c = 2 \frac{\omega_0}{Q_e} \frac{dV_F}{dt} - \frac{\omega_0}{2} \left[\frac{R}{Q} \right] \frac{dI_b}{dt}, \quad (1)$$

where $\omega_0 = 1/\sqrt{LC}$ is the resonant frequency of the cavity, $Q_L(Q_e)$ is the loaded (external) quality factor of the cavity, and $V_c = V_F + V_R$ is the cavity voltage which is the sum of the forward and reverse voltages. Here,

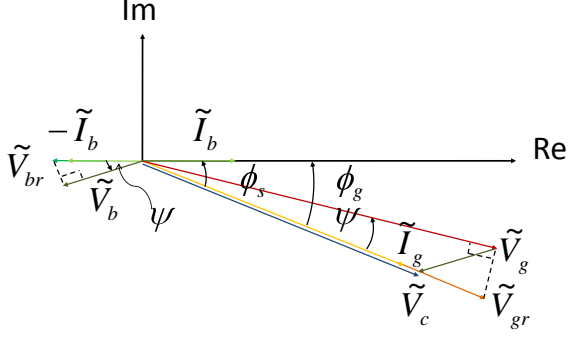


FIG. 3: Phasor diagram used to calculate tuning angle ψ needed to make the cavity voltage \tilde{V}_c and generator current \tilde{I}_g in phase.

$\Delta[1/Q]$ denotes the change in the quality factor due to Ohmic dissipation, and $[R/Q]$ is the beam-coupling parameter. Negative sign in front of the beam current I_b indicates that the induced voltage from the beam current will decelerate the beam. Let's take the each term to be varying at roughly the driving frequency ω and express it in terms of phasor:

$$V = \text{Re} \left[\tilde{V}(t) e^{j\omega t} \right]. \quad (2)$$

Here, we allow for some slow variation in the envelopes. In the slowly-varying envelope approximation, $|d\tilde{V}/dt| \ll |\omega\tilde{V}|$, the cavity responds to the generator and beam currents according to

$$\frac{d\tilde{V}_c}{d\tau} + (1 - j \tan \psi + \gamma)\tilde{V}_c = \frac{1}{2} Q_L \left[\frac{R}{Q} \right] (\tilde{I}_g - \tilde{I}_b). \quad (3)$$

Here, $\tau = t/T_f$ is time measured in units of filling time $T_f = 2Q_L/\omega_0$, and $\gamma = Q_L \Delta[1/Q]$ is a damping coefficient. The difference in driving frequency from resonant frequency is characterized by tuning angle ψ , which is given by

$$\tan \psi = Q_L \left(\frac{\omega_0}{\omega} - \frac{\omega}{\omega_0} \right). \quad (4)$$

III. LOADING FROM BEAM-INDUCED IMAGE CHARGES

The average DC beam current is given by

$$I_{DC} = \frac{q_b}{T_b}. \quad (5)$$

Here, q_b is the total charge in one bunch and T_b is bunch spacing which is usually a sub-harmonic of the fundamental mode frequency (e.g., $T_b = 4/f = 5$ ns for the

HPRF). For typical beam intensity expected in the Fermilab linac ($\sim 10^9$ proton/bunch), we expect $I_{DC} \approx 32$ mA. Considering the bunch length (≈ 0.13 ns) is much smaller than the bunch spacing (≈ 5 ns), we can treat each bunch as a delta function-like pulse and obtain the Fourier component of the beam current as $\tilde{I}_b = 2I_{DC}$. In steady state with $\gamma = 0$, the beam-induced voltage from \tilde{I}_b becomes

$$\tilde{V}_b = -\cos \psi e^{j\psi} Q_L \left[\frac{R}{Q} \right] I_{DC} = \tilde{V}_{br} \cos \psi e^{j\psi}, \quad (6)$$

where \tilde{V}_{br} is the beam-induced voltage at resonance ($\psi = 0$). If \tilde{V}_b is non-negligible compared with the cavity voltage \tilde{V}_c , then the cavity no longer appears to the generator purely resistive. In this case, adjustment of tuning angle $\psi (\neq 0)$ is required to get the cavity voltage \tilde{V}_c and generator current \tilde{I}_g in phase, maximizing the energy flow from the generator to the cavity. Consequently, the required frequency detuning is given by

$$\delta f = f_0 - f = \frac{f_0}{2Q_L} \frac{|\tilde{V}_{br}|}{|\tilde{V}_c|} \sin \phi_s. \quad (7)$$

Here, ϕ_s is the angle between the beam current phasor and the cavity voltage phasor (synchronous phase). To estimate δf , we consider a simple pill box cavity with radius r_w and axial length d , in which $[R/Q] \approx (\mu_0/\epsilon_0)^{1/2} \times T^2(d/r_w)$, transit-time factor $T = \sin(\pi d/\beta\lambda)/(\pi d/\beta\lambda)$, $|\tilde{V}_c| \approx E_0 T d$. If we take the parameters to be $r_w = 11.43$ cm, $d = 3$ cm, $E_0 = 20$ MV/m, $f_0 = 805$ MHz, $Q_L = 6000$, $\beta = v/c = 0.57$, $\phi_s = 32^\circ$, and $\lambda = c/f_0 = 37$ cm, we have $|\tilde{V}_{br}| \sim 18$ kV, $|\tilde{V}_c| \sim 580$ kV, and $\delta f \sim 1.0$ kHz. Hence, the required detuning δf is small compared with the half-bandwidth of the resonant cavity $f_0/2Q_L \sim 67$ kHz, implying that the loading effect from the beam itself will not change the resonance frequency significantly.

Other aspect we may consider is the coupling coefficient β_c . Normally, we adjust the power coupler so that the cavity is matched to the generator (critical coupling, $\beta_c = 1$), resulting in zero reflected power at steady state. In this way, we can minimize the generator power required to get a certain cavity voltage at steady state. When beam is present in the cavity, however, the beam not only absorbs some amount of generator power but also causes power reflection, wasting some additional generator power. The adjustment of the coupler needed for minimum reflected power is given by

$$\delta\beta_c = \frac{P_b}{P_w}, \quad (8)$$

where $P_b = |\tilde{V}_c| I_{DC} \cos \phi_s$ is the average power delivered to the beam, and $P_w = |\tilde{V}_c|^2/R_{sh}$ is the power dissipated on the cavity wall with effective shunt impedance $R_{sh} = 2Q_L [R/Q]$. Considering the typical HPRF cavity parameters, we find $P_b \sim 16$ kW, $P_w \sim 303$ kW, and $\delta\beta_c \sim 0.05$.

Hence, from simple estimations based on Eqs. (7) and (8), we expect that the loading effect from beam-induced image charges is quite small, at least compared with the effect of beam-induced electrons (will be discussed in next section).

IV. LOADING FROM BEAM-INDUCED ELECTRONS

A. Electron generation and evolution

During propagation through the hydrogen gas, the incident beam generates electrons by beam-impact ionization. The electrons ejected from the primary ionization also produce some secondary electron/ion pairs. The resultant increase in the electron density after one micropulse ($\sim 10^9$ protons) passes through the cavity can be conveniently expressed by

$$\Delta n_e \approx \frac{1}{\pi r_b^2} \frac{\rho dE/dx}{W_i} \times 10^9, \quad (9)$$

where r_b (≈ 1 cm) is the radius of a uniform density beam, ρ [g/cm^3] $\approx 5.6 \times 10^{-6} p$ [psi] is the mass density of hydrogen gas at room temperature $T_{\text{room}} = 300$ K, dE/dx is the stopping power, and W_i ($= 35$ eV) is the effective average energy to produce an electron/ion pair.

Most electrons are thermalized quickly by elastic and inelastic collisions with background hydrogen gas, and drift with the applied RF field until annihilated through recombination, attachment, or diffusion. The electron equilibrium energy is approximately given by

$$\bar{\epsilon} = \frac{3}{2} T_e \approx 0.357 \times \left(\frac{E_{rms}}{p} \right)^{0.71}, \quad (10)$$

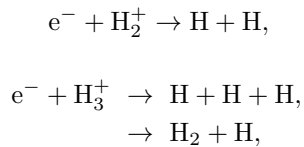
where $\bar{\epsilon}$ and T_e are in eV, $E_{rms} = E_0/\sqrt{2}$ is in V/cm, and p is in torr. A simplified rate equation for the electron density in thermal equilibrium can be written as

$$\frac{dn_e}{dt} = S - \beta_r(T_e)n_e^2 - k_a(T_e, T_{\text{H}_2})n_e n_{\text{H}_2} - \frac{D(T_e)}{\Lambda^2} n_e. \quad (11)$$

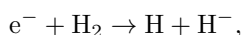
Here, S is the average source term which is defined as

$$S \approx \frac{\Delta n_e}{T_b}, \quad (12)$$

β_r is the (total) rate coefficient for dissociative recombination (DR) processes, such as



k_a is the rate coefficient for dissociative attachment (DA) to background hydrogen gas,



and D and Λ are diffusion coefficient and length respectively. At high pressure considered in the study, diffusion is often negligible. Since only the lowest vibrational level of the ground electronic state of H_2 is populated at room temperature, we expect $k_a \lesssim 10^{-14} \text{ cm}^3 \text{ s}^{-1}$. Therefore, in this section, we consider only the recombination process in solving Eq. (11). Possible enhancement of dissociative attachment rate due to vibrational excitation will be discussed in Sec. VI.

Figure 4 illustrates the evolutions of the electron density with several different macropulse lengths and beam intensities. Here, beam pulse is assumed to arrive at the cavity at $t = 0$. It is clear that electron accumulation saturates to some finite level due to the recombination process, particularly for long bunch length cases. When the beam is off, then there is no electron source, and the electron density decays slowly with characteristic time scale of $\tau_r \sim (n_e \beta_r)^{-1}$.

B. Perturbations from electrons

For the nominal operating conditions of the HPRF cavity ($f = \omega/2\pi \approx 805$ MHz), ions can be assumed to be immobile. On the other hand, electrons not only interact with the external RF field, but also suffer collisions with background gas molecules. The total electron-neutral collision frequency for momentum transfer is approximately given $\nu_m \approx 2.3 \times 10^{11} p$ [psi] for $4 < E_0/p$ [V/cm/torr] < 30 and $T_{\text{room}} = 300$ K, and the response of plasma electrons to the external RF field is described by conductivity:

$$\sigma = \sigma_{DC} \left[\frac{\nu_m^2}{\nu_m^2 + \omega^2} + j \frac{\omega \nu_m}{\nu_m^2 + \omega^2} \right], \quad (13)$$

where $\sigma_{DC} = n_e e^2 / m_e \nu_m$ is the DC conductivity. When the cavity is (partially) filled with electrons of complex conductivity (13), the imaginary part causes the shift in the resonance frequency and the real part the decrease in the Q value. They are given by Slater's perturbation equations as

$$\Delta f = f_0 - f \approx \frac{f_0}{2} \left(\frac{\omega_0}{\nu_m} \right) \Delta \left[\frac{1}{Q} \right], \quad (14)$$

$$\Delta \left[\frac{1}{Q} \right] \approx \frac{\int_V \frac{1}{2} \sigma_{DC} E_0^2(r, z) dV}{\omega_0 \int_V \frac{1}{2} \epsilon_0 E_0^2(r, z) dV} = \left(\frac{\omega_0}{\nu_m} \right) \frac{\langle n_e \rangle}{n_c}, \quad (15)$$

where $\langle n_e \rangle = \int_V n_e E_0^2 dV / \int_V E_0^2 dV$ is the average electron density weighted over initial spatial electric field distribution $E_0(r, z)$, and $n_c = \epsilon_0 m_e \omega_0^2 / e^2$ is the critical density. If the electron swarm consists of a small radius uniform column ($r \approx r_b$), much smaller than the cavity radius r_w , then we can further approximate $\langle n_e \rangle \approx n_e (\xi r_b^2 / r_w^2)$, where the geometric factor ξ indicates that the effect of accumulated electrons is large at places where E_0 is large. For example, $\xi = 1$ when the

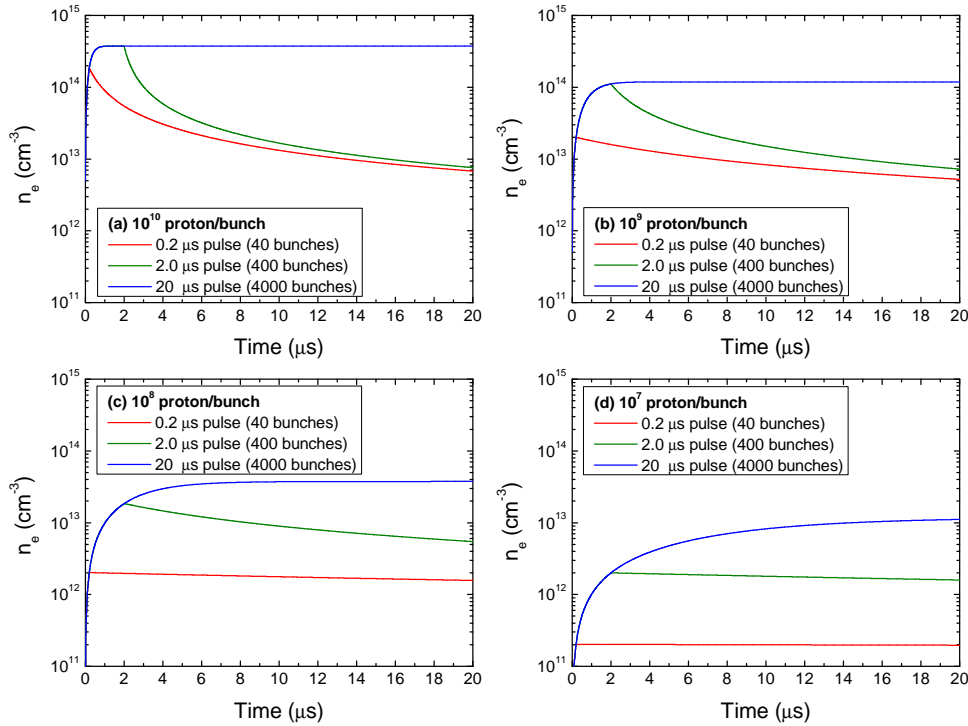


FIG. 4: Plots of electron density evolution with different macropulse lengths and beam intensities estimated from Eq. (11). Here, $E_0 = 20$ MV/m, $p = 1000$ psi, and $T_b = 5$ ns. For recombination rate coefficient we assume $\beta_r \sim 7 \times 10^{-9} \text{cm}^3/\text{s}$

electric field is uniform across the cavity, while $\xi = 3.71$ for the case of a simple pillbox cavity. In the actual HPRF cavity, electric fields are highly concentrated near the center where most electrons are expected to be accumulated, therefore, the value of ξ will become even higher. It should be emphasized here that Eqs. (14) and (15) are derived based on the small perturbation. Hence, their accuracy is questionable (particularly for frequency shift) when electron density becomes too high. Note that $n_e \propto \rho \propto p$, therefore, $\Delta[1/Q]$ is independent of pressure as long as $\nu_m \propto p$ (which is not true, particularly for $E_0/p \lesssim 4$). For lower values of E_0/p , there exists some nonlinearity in the relation between ν_m and p , which enhances Ohmic dissipation and resultant changes in the cavity quality factor.

C. Changes in the pickup signal

With no beam current ($\tilde{I}_b = 0$), zero detuning ($\psi = 0$), and proper normalization [for $\gamma \rightarrow 0$, $\hat{V}_c(t \rightarrow \infty) \rightarrow 1$], Eq. (3) is simplified as

$$\frac{d\hat{V}_c}{d\tau} + [1 + \gamma(\tau)] \hat{V}_c = 1. \quad (16)$$

Here, the damping coefficient γ is essentially the ratio of power dissipated by Ohmic heating by electrons (P_{Ohmic}) to power dissipated in the cavity wall (P_{wall}) and the external load (P_{ext}), i.e., $\gamma = P_{\text{Ohmic}}/(P_{\text{wall}} + P_{\text{ext}})$. Note that γ is directly proportional to the evolution of electron density. When there is significant reduction in the pickup signal as indicated in Fig. 5, the electron temperature will be lowered and the recombination rate will be increased accordingly. Indeed, this effect may cause the pickup signal to recover much quicker than expected in Fig. 5.

When there is significant change in the resonant frequency, we cannot simply neglect the detuning term ($j \tan \psi$) in Eq. (3). This detuning effect will not only further reduce the amplitude of the pickup signal, but also cause phase shift in both pickup and reflected signals.

V. SUPERFISH CALCULATION

SUPERFISH is a freeware program for calculating RF fields in either 2-D cartesian coordinates or axially symmetric cylindrical coordinates. Although SUPERFISH itself cannot handle the microscopic electron dynamics with collisions and various molecular processes, average

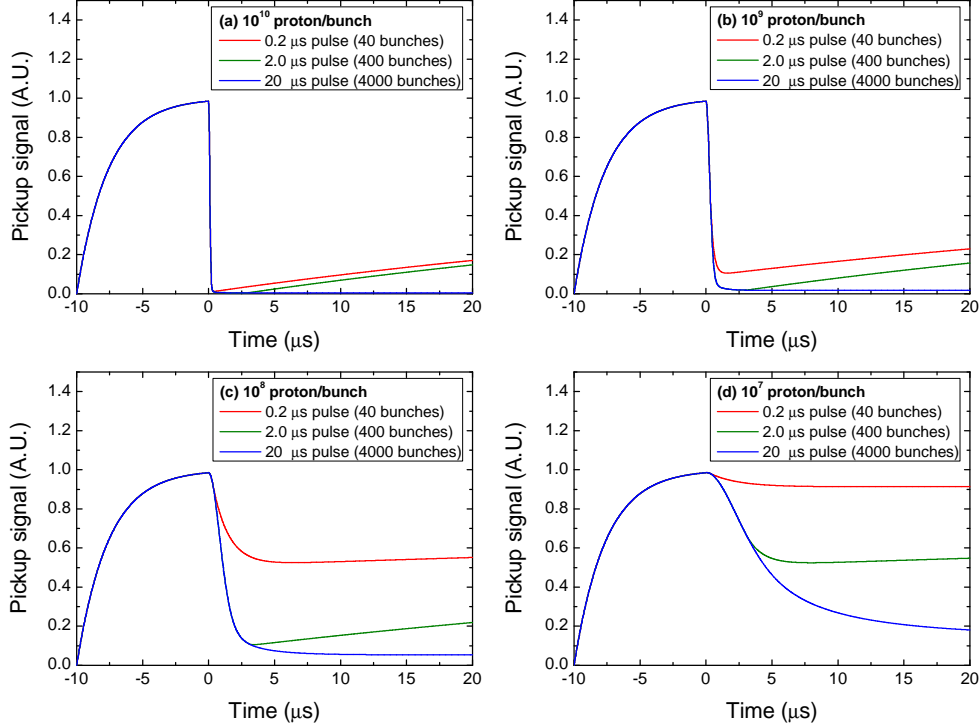


FIG. 5: Plots of changes in the amplitude of the pickup signal with different macropulse lengths and beam intensities. Here, $E_0 = 20$ MV/m, $p = 1000$ psi, $T_b = 5$ ns, and $Q_L = 6000$. For simplicity, a simple pill box cavity without detuning has been assumed. The RF pulse starts at $t = -10$ μ s and ends $t = 20$ μ s while incident beam is on at $t = 0$ μ s.

macroscopic effects can be calculated by using appropriate dielectric constant.

A. Changes due to high pressure gas

When the cavity is pressurized, we observe changes in the resonance frequency mostly due to the increase in the electric susceptibility χ_e (See Fig. 6). Using the approximate relation between susceptibility (the macroscopic parameter) and molecular polarizability (the microscopic parameter), we obtain the following dielectric constant that includes the presence of high pressure gas:

$$\epsilon/\epsilon_0 = 1 + \chi_e = 1 + \frac{(n\alpha_p/\epsilon_0)}{1 - (n\alpha_p/3\epsilon_0)}. \quad (17)$$

Here, α_p is molecular polarizability, which is often expressed in terms of relative polarizability $\alpha_R = \alpha_p/(4\pi\epsilon_0 a_0^3)$, where a_0 is the Bohr radius. Note that number density of the gas n is proportional to the gas pressure by $n[\text{cm}^{-3}] \approx 1.7 \times 10^{18} p[\text{psi}]$.

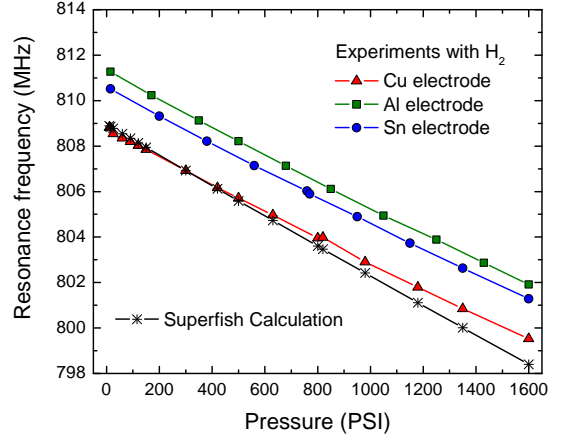


FIG. 6: Changes in the resonance frequency according to the hydrogen gas pressure.

B. Changes due to electrons

When electrons are accumulated inside the cavity, the electron column can be regarded as a lossy dielec-

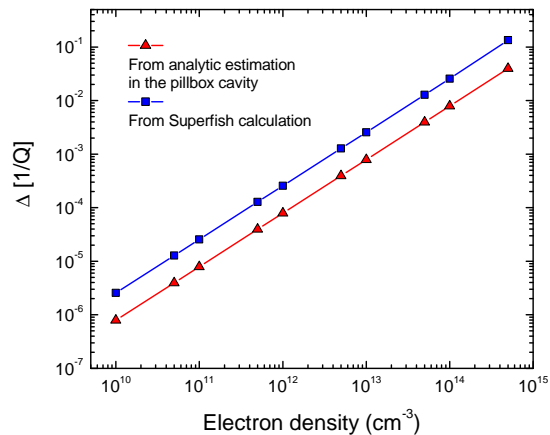


FIG. 7: Changes in the quality factor depending on the electron density.

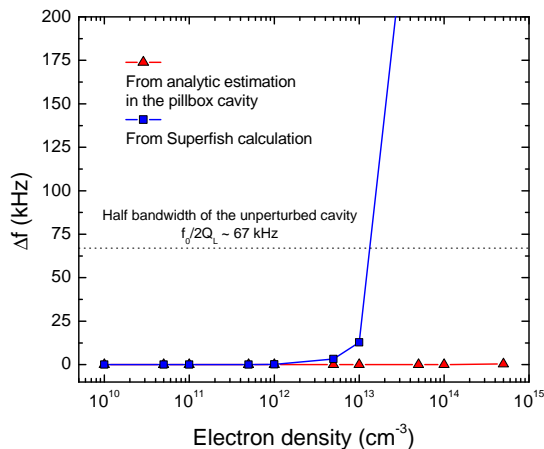


FIG. 8: Changes in the resonance frequency depending on the electron density.

tric material with complex dielectric constant. Using the plasma conductivity defined in Eq. (13), we find $\epsilon/\epsilon_0 = 1 - j\sigma/(\epsilon_0\omega)$, or explicitly,

$$\epsilon/\epsilon_0 = 1 - \frac{\omega_{pe}^2}{\nu_m^2 + \omega^2} + j \left(\frac{\nu_m}{\omega} \right) \frac{\omega_{pe}^2}{\nu_m^2 + \omega^2}, \quad (18)$$

where $\omega_{pe}^2 = n_e e^2 / (\epsilon_0 m_e)$ is the plasma frequency.

Figure 7 shows the changes in the quality factor $\Delta[1/Q]$ calculated either from simple analytic formula (15) in the pill box configuration or SUPERFISH in the actual HPRF cavity. The discrepancy between those two calculations are attributed to the geometric effect explained in Sec. IV B. Apart from the factor ~ 3 , both calculations exhibit a linear relation between $\Delta[1/Q]$ and electron density as expected.

On the other hand, values of the resonance frequency

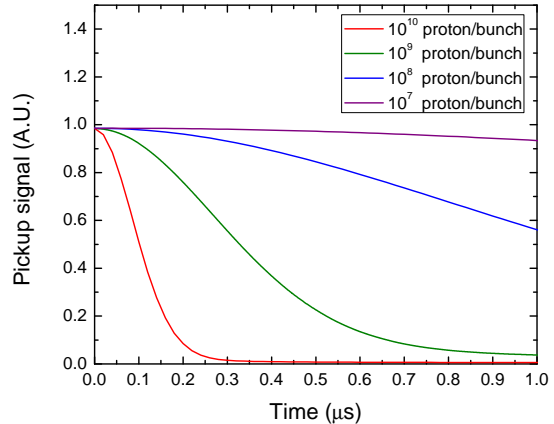


FIG. 9: Changes in the amplitude of the pickup signal right after beam is incident on the cavity. The decay time is expected to be somewhat longer than the typical gas breakdown time scale (~ 20 ns) observed in the previous experiment. Note that, however, shift in the resonance frequency is not included in this plot.

shift Δf are quite different depending on the calculation methods. While Δf appears to be negligibly small in the analytic estimation, SUPERFISH calculation indicates that Δf increases considerably after $n_e > 10^{13} \text{cm}^{-3}$. It is suspected that perturbation method for calculating resonance frequency is no longer valid after electric fields are violently altered. If $\Delta f > f_0/2Q_L$, we may observe phase shift in the pickup signal as well.

VI. EXPERIMENTS

A. Scan for different macropulse length and beam intensity

How to change either macropulse length or beam intensity without affecting whole accelerator complex should be discussed in detail before beam commissioning. Such capability is vital for the successful physics program of the HPRF beam test.

For currently envisioned beam parameters ($\sim 10^9$ proton/bunch and $\sim 20 \mu\text{s}$ macropulse length), we expect fast decay of the pickup signal and huge reflected power (see. Fig. 5). Even in this case, the decay time may be somewhat longer than typical gas breakdown time scale (~ 20 ns) observed in the previous experiment (See. Fig. 9).

With long RF pulse ($> 60 \mu\text{s}$), we may investigate the effect of recombination (or other electron removal process) by observing recovery of the pickup signal after beam passes through the cavity.

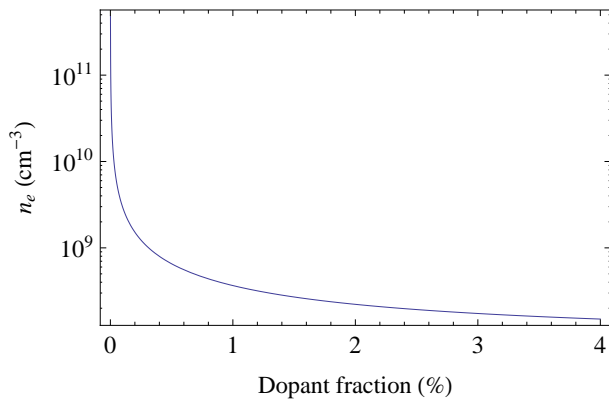


FIG. 10: Equilibrium electron density as a function of dopant fraction for the case of $\sim 10^9$ proton/bunch.

B. Scan for different E_0/p

As long as E_0/p is less than the gas breakdown limit, operating HPRF cavity at higher E_0/p seems to be more favorable for dissociative attachment. At higher E_0/p , the heating of a hydrogen molecule by collisions with electrons will increase, and the vibrational excitation of the ground state molecule could be enhanced. The dissocia-

tive attachment rate is known to increase dramatically with increasing vibrational energy.

In addition, electrons with higher E_0/p tends to have the higher dissociative attachment rate for a given vibrational state.

C. Scan for different dopant gas fraction

With a dopant gas, the average lifetime of a beam-induced electron is determined by the sum of the time needed for the electron to be thermalized to an energy level at which attachment becomes significant, τ_ϵ , plus the average time required before the electron is then captured, $\tau_a \approx 1/(k_a \alpha n)$. Here, k_a is the electron attachment rate coefficient and α is the partial fraction of dopant in the gas mixture. If $\tau_\epsilon + \tau_a < T_b (= 5 \text{ ns})$, then the equilibrium electron density is approximately given by

$$n_e \approx S(\tau_\epsilon + \tau_a). \quad (19)$$

Figure 10 suggests that dopant fraction of only $\sim 0.2\%$ is enough to minimize the beam loading effect presented in Figs. 4 and 5.